Received 21 July 2023; revised 6 September 2023; accepted 13 September 2023. Date of publication 15 September 2023; date of current version 9 October 2023.
The review of this article was arranged by Editor Z. Zhang.

Digital Object Identifier 10.1109/JEDS.2023.3316355

2-Mercaptobutanedioic-Acid-Modified AlGaN/GaN High Electron Mobility Transistor With Folded Gate for Fe^{3+} Detection

YAN GU[1], XUECHENG JIANG[1], NAIYAN LU[1], JIARUI GUO[1], YUSHEN LIU[2], XIFENG YANG[2], WEIYING QIAN[1], XIANGYANG ZHANG[1], GUOQING CHEN[1], TAO TAO[3], AND GUOFENG YANG[1] (Member, IEEE)

1 School of Science, Jiangsu Provincial Research Center of Light Industrial Optoelectronic Engineering and Technology, Jiangnan University, Wuxi 214122, China
2 College of Electronic and Information Engineering, Changshu Institute of Technology, Changshu 215500, China
3 School of Electronic Science and Engineering, Nanjing University, Nanjing 210093, China

CORRESPONDING AUTHORS: W. QIAN AND G. YANG (e-mail: 372110007@qq.com; gfyang@jiangnan.edu.cn)

This work was supported in part by the National Natural Science Foundation of China under Grant 61974056, Grant 62174016, Grant 62074019, and Grant 62104084; in part by the Key Research and Development Program of Jiangsu Province under Grant BE2020756; in part by the Suzhou Science and Technology Project under Grant SZS2020313; and in part by the Fundamental Research Funds for Central Universities under Grant JUSRP22032.

ABSTRACT A 2-mercaptobutanedioic acid modified enhancement-mode AlGaN/GaN high-electron-mobility transistor (HEMT) device with a 5-fold gate was proposed for Fe^{3+} specific detection. The crystal quality and surface morphology of the epitaxial material were characterized by X-ray diffraction and atomic force microscopy. The analysis of I-V characteristics and the current response of the device at a constant drain bias of 7 V show that the current response variation increased with an increase in Fe^{3+} concentration. Additionally, the sensitivity of the 5-fold-gate HEMT sensor was calculated, which was found to be greater. The current response results of the HEMT after adding multiple heavy metal ions proved that the sensor specifically recognizes Fe^{3+}. Therefore, the 2-mercaptobutanedioic acid modified 5-fold gate HEMT sensor has great potential in the real-time detection of trace Fe^{3+}.

INDEX TERMS Enhancement-mode HEMT, sensor, surface modification, iron ion.

I. INTRODUCTION

With advancements in science and technology and the rapid development of industrialization, increasing levels of human activity, including mining, industry, agriculture, and metallurgy, have escalated the accumulation of heavy metal ions in the human living environment [1], [2]. These additional heavy metal ions are collected continuously in the air, water, and soil, as well as in plants and animals on the earth's surface [3]. Owing to the lack of natural degradability of heavy metal elements, consumption of such polluted plants, animals, and water would cause the transfer of heavy metals to the human body and subsequent gradual accumulation [4]. Although heavy metals, such as calcium and zinc, in appropriate concentrations, play a crucial role in maintaining normal physiological processes and healthy development in the human body, excessive intake or accumulation of these elements would cause irreversible damage to the human body [5]. When the human body accumulates iron ions (Fe^{3+}) at levels deviating from the normal range, it can lead to functional disorders and various diseases, such as heart failure, hemosiderosis, and neurodegeneration [6], [7]. Currently, mature detection methods for Fe^{3+} require large equipment and complex experimental procedures in a laboratory environment, as well as specialized training for the personnel [8], [9]. Therefore, the device that is sophisticated, simple to operate, efficient, and highly sensitive for detecting Fe^{3+} has become a focal point of attention.

In recent years, AlGaN/GaN materials have been widely applied in optoelectronic detectors [10], chemical sensors, and power electronics [11], [12], [13], [14], [15], [16] due to their high-electron-mobility, high breakdown field strength, and good resistance to high-temperature and corrosion [17], [18], [19], [20]. Therefore, sensors based on AlGaN/GaN high-electron-mobility transistors (HEMTs) have the potential for ion detection. Niu et al. considered the principle that led ions to generate positive potential on the gold gate of the

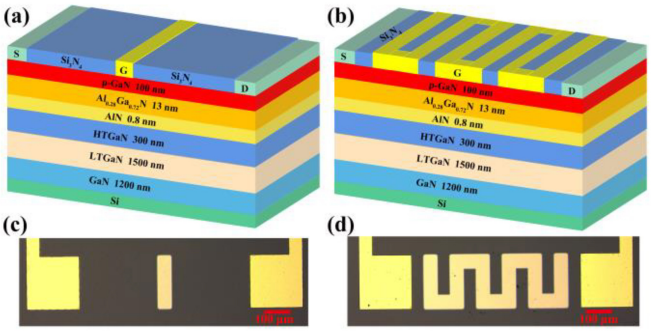

FIGURE 1. **Structure of a high-electron-mobility transistor with (a) a conventional and (b) a 5-fold gate (HT: high-temperature; LT: low-temperature). Top-view optical micrographs of (c) a traditional and (d) a folded gate.**

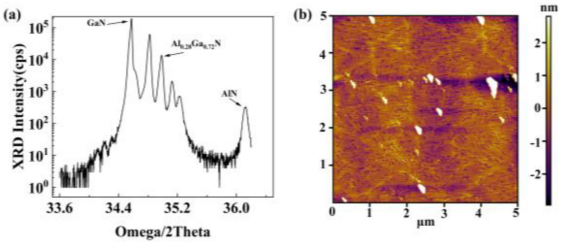

FIGURE 2. **(a) X-ray diffraction (0002) ω-2θ scan of epitaxial material. (b) 5 μm × 5 μm atomic force micrograph of the p-type GaN layer.**

pseudomorphic high-electron-mobility transistor (pHEMT) sensor and increase the current between the source and drain. Besides, they functionalized glutathione on the gold-plated gate area of pHEMT, realizing the detection of trace Pb^{2+} [21]. For zinc ion detection, L. Gu et al. developed a Schiff base functionalized AlGaN/GaN HEMT sensor, producing a fast response of less than 10 s over the range of 1 fM to 1 μM in zinc ion concentration [22].

Conventional HEMTs require a negative bias voltage to be applied to their gate region for controlling the two-dimensional electron gas (2DEG) concentration and achieving device on/off switching [23], which places high demands on the control circuit in practical applications. An enhancement-mode AlGaN/GaN HEMT with a p-type GaN cap layer is proposed. This type of device raises the threshold voltage by depleting the 2DEG at the heterojunction channel, enabling the sensor to be switched on/off with a positive gate voltage [24].

In this work, enhancement-mode AlGaN/GaN HEMTs with conventional and 5-fold gate structures were fabricated to investigate their performance in Fe^{3+} detection. 2-mercaptobutanedioic acid was selected as the modifying material to stabilize the detection of Fe^{3+} [25]. Experimental results showed that, compared with the conventional structure, the 5-fold-gate sensor had higher sensitivity and specificity for Fe^{3+} detection. This demonstrates its great development prospects in the field of efficient and highly sensitive detection equipment.

II. DEVICE FABRICATION AND EXPERIMENTAL DETAILS

Figure 1(a) schematizes an enhancement-mode AlGaN/GaN HEMT with a traditional structure, with a rectangular gate length and width of 50 μm and 200 μm, respectively. The epitaxial structure deposited on a silicon substrate includes a 1200-nm-thick GaN nucleation layer, a 1500-nm-thick low-temperature GaN buffer layer, a 300-nm-thick undoped high-temperature GaN channel layer, a 0.8-nm-thick AlN spacer layer, a 13-nm-thick $Al_{0.28}Ga_{0.72}N$ barrier layer, and a 100-nm-thick p-type GaN cap layer.

After fabricating the epitaxial structure, inductively coupled plasma was used for the surface treatment to isolate each device and the source/drain regions. The metal stack for ohmic contacts was formed by the electron beam evaporation deposition of Cr/Al/Ti/Pt/Au (1.5/120/75/50/1500 nm) according to the designed photomask pattern, followed by high-temperature annealing for 30 s in a nitrogen gas flow, resulting in a symmetric 200-μm-wide and 650-μm-spaced source/drain electrode structure. The device was then passivated with a 250-nm-thick Si_3N_4 layer, followed by etching of the gate electrode area and electron beam evaporation deposition of a 50-nm-thick Au layer onto it.

Figure 1(b) illustrates the structure of a 5-fold-gate HEMT with an effective gate area of 72,500 μm^2. Figure 1(c) and (d) compare the top-view optical microscope images of the traditional and 5-fold gate structures, respectively.

The fabricated devices were characterized by X-ray diffraction (XRD) and atomic force microscopy (AFM). The XRD (0002) ω-2θ scan pattern (Figure 2(a)) exhibited characteristic peaks at 34.58°, 34.98°, and 36.12°, corresponding to the GaN, AlGaN, and AlN layers, respectively. Besides, the peaks of LT GaN and HT GaN have shifted due to changes in lattice constant caused by the stress modification. The stoichiometric Al content in the AlGaN layer was confirmed to be 0.28. Figure 2(b) shows an AFM image of the p-type GaN surface, revealing a root-mean-square roughness of 1.596 nm in a scan range of 5 μm × 5 μm. The GaN surface also showed a step-like morphology, indicating its integrity and stability; thus, it met the requirements of morphology and composition for epitaxial growth.

After confirming the device composition, the surface modification process was performed. A 5-g/L solution of 2-mercaptobutanoic acid was continuously dropped onto the gate surface for 1 h, followed by 12-h static incubation at room temperature. Due to the strong interaction between the gold film on the gate surface and the thiol group of 2-mercaptobutanoic acid, Au–S coordination bonds were formed, allowing the 2-mercaptobutanoic acid molecules to easily self-assemble on the gold film and achieve surface functionalization [26].

III. RESULTS AND DISCUSSION

The proposed enhancement-mode HEMT requires a certain forward bias to be applied to the gate surface to activate the

2DEG channel at the AlGaN/GaN heterojunction interface, achieving carrier conduction. As a result, after adding different concentrations of heavy metal ions, the drain current (I_d) of the device can be detected by a probe station as a function of the gate potential (V_g). The relationship between the carrier density of the 2DEG channel (n_s) and V_g can be explained as follows [27], [28]:

$$n_s = \frac{\varepsilon_n}{qd}\left(V_g - V_t - V(x)\right) \tag{1}$$

where ε_n is the permittivity of the AlGaN barrier layer, q is the electronic charge, d is the distance from the 2DEG channel to the surface, and V_t and $V(x)$ are, respectively, the threshold voltage and the channel potential. The opening and closing of the 2DEG channel are directly controlled by V_g and are highly sensitive. The I_d of the AlGaN/GaN HEMT can be expressed as a function of V_g as follows [29]:

$$I_d = \frac{\varepsilon_n \mu W}{2dL}\left[2\left(V_g - V_t\right)V_d - V_d^2\right] \tag{2}$$

where μ is the carrier mobility in the 2DEG, V_d is the drain bias, and W and L are, respectively, the width and length of the functionalized gate region. When V_d is constant, the variation of the gate surface charge directly affects the I_d.

The specific working process of the enhancement-mode HEMT realized by the addition of a p-GaN cap layer can be characterized by three stages. The built-in voltage of the p-GaN capping layer and AlGaN barrier layer is recorded as V_f. When the gate bias is initially applied at less than the threshold voltage ($0\ V < V_g < V_t$), the bottom of the conduction band at the AlGaN/GaN position is higher than the Fermi level. Thus, the 2DEG channel is not turned on, and the device remains in the off state. As the gate voltage increases and is higher than the threshold voltage and lower than the built-in voltage ($V_t < V_g < V_f$), the bottom of the heterojunction conduction band is lower than the Fermi level, the 2DEG channel is turned on, and the device is in the on the state. At this stage, there are fewer carriers in the channel, indicating that the drain current of the device is smaller. When the gate bias voltage is gradually increased to a voltage greater than the built-in voltage ($V_g > V_f$), under the action of the gate electric field, a large number of holes in the p-GaN capping layer accumulate in the 2DEG channel corresponding to the gate position. Additionally, a large number of electrons are induced from the source to gather there. These attracted electrons will drift under the applied drain bias, resulting in a stronger source-drain current.

The I–V characteristics of AlGaN/GaN HEMT sensors with different gate structures were measured by applying a 0–10 V drain bias to the sensors under different concentrations of Fe^{3+}. The measurements were carried out using a probe station equipped with a Keithley SCS-4200 parameter analyzer. Figure 3(a) shows the I–V characteristics of enhancement-mode HEMT devices with a conventional gate structure. At a drain voltage less than 2 V, the current of the device increased slowly, gradually increasing in different magnitudes above 2 V and continuing to rise until reaching

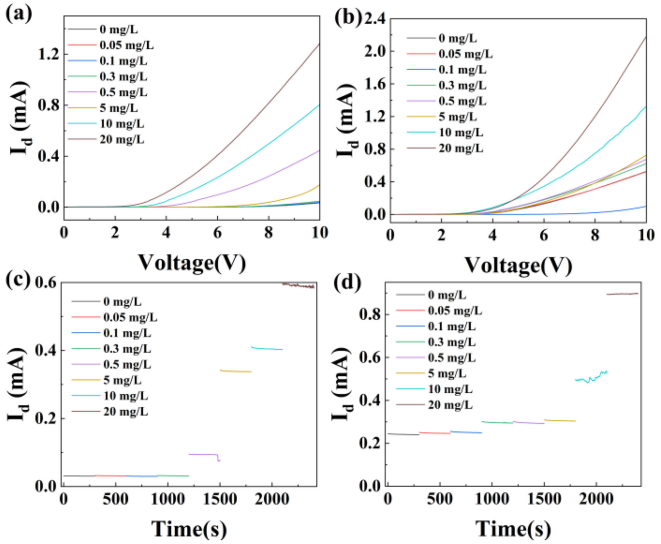

FIGURE 3. I–V characteristics of the enhancement-mode HEMT sensor with a (a) conventional gate and (b) 5-fold gate; current response of the enhancement-mode HEMT sensor with a (c) conventional gate and (d) 5-fold gate.

an applied bias voltage of 10 V. At 10 V, the minimum and maximum drain currents of the enhancement-mode HEMT devices with traditional gate structure were 0.047 mA and 1.29 mA, respectively, obtained by measuring with a blank solution (0 mg/L) and 20 mg/L Fe^{3+} solution. The I–V curves of the devices measured with Fe^{3+} concentrations less than 5 mg/L were almost identical to those measured with the blank solution, with very slightly elevated values. The I–V curves of the enhancement-mode HEMT devices measured with Fe^{3+} concentrations greater than or equal to 5 mg/L showed considerable differences in the increase of the magnitude of drain current, as the current increased with an increase in the ion concentration.

In this experiment, enhancement-mode HEMT devices were selected, and a certain forward bias voltage was applied to the gate surface to facilitate the opening of the 2DEG channel at the AlGaN/GaN heterojunction interface and achieve carrier conduction, such that changes in the drain current with increasing drain voltage could be detected through a probe station. This enabled the analysis of the I–V curve of the device. Adding Fe^{3+} solution to the gate surface produces a 2-mercaptobutanoic acid molecular film, and Fe^{3+} combines with its carboxyl group to form complexes, which increases the surface potential, equivalent to applying a forward bias voltage to the gate surface. However, when the added Fe^{3+} concentration was less than 0.5 mg/L, the potential raised on the gate surface was not sufficient to meet the standard for opening the 2DEG channel. After the addition of a concentration greater than 0.5 mg/L, the 2DEG channel is opened. As the concentration of introduced Fe^{3+} gradually increased, the gate potential gradually increased with the increase of the carrier density in the 2DEG channel, resulting in a considerable increase in the detected drain current.

Figure 3(b) shows the I–V characteristic curves of the enhancement-mode HEMT device with 5-fold gates, demonstrating a curve trend similar to that of the conventional gate HEMT device. The current gradually increases above the 2 V bias voltage. Under a drain voltage of 10 V, the minimum drain current of the device in this structure is 0.10 mA for 0.1 mg/L Fe^{3+}, and the maximum current value is 2.18 mA for 20 mg/L Fe^{3+}, both of which are higher than that of the HEMT device with a conventional gate at the corresponding concentrations. The I–V curves with Fe^{3+} concentrations higher than 0.1 mg/L show a different growth trend than that of the blank solution. Therefore, during the process of combining the Fe^{3+} solution with the 2-mercaptobutanoic acid molecular film on the surface of the 5-fold-gate HEMT device to form complexes, the increased gate potential satisfies the conduction conditions of the 2DEG channel, realizing the detection of Fe^{3+}. As the gate area increases, the effective surface area of the enhancement-mode HEMT device that can interact with the measured ions increases. This further increases the gate potential, which is equivalent to applying a gate bias voltage, reducing the required ion concentration for opening the 2DEG channel. In addition, the electric field near the channel can be continuously superimposed, which enables to obtain a larger current response. This means that the lower limit of the real-time measured ion concentration is reduced.

The two types of fabricated enhancement-mode HEMTs exhibited differentiated current responses to varying concentrations of Fe^{3+} under a constant V_d. Figure 3(c) shows the I_d response within 300 s of the device with the traditional gate structure to Fe^{3+} concentrations ranging from 0 to 20 mg/L at a V_d of 7 V. The minimum and maximum I_d of the sensor with a traditional gate structure were 0.031 mA (at 0 mg/L Fe^{3+}) and 0.594 mA (at 20 mg/L Fe^{3+}), respectively. At each Fe^{3+} concentration, the current response remained relatively stable during the test period (300 s). However, it gradually increased along with the Fe^{3+} concentration; this happened because the introduced Fe^{3+} formed complexes with the 2-mercaptobutyric acid molecules on the gate layer, changing the polarity of the HEMT surface and increasing its positive charge. According to Equations (1) and (2), an increase in surface potential leads to an increase in the charge density of the 2DEG channel, enhancing the I_d detection. The current response within the Fe^{3+} concentration range of 0–0.3 mg/L did not significantly increase, possibly because the surface potential increase was not sufficient to open the 2DEG channel. Figure 3(d) displays the current response of the HEMT with a 5-fold gate at a V_d of 7 V, which showed a maximum I_d of 0.903 mA (at 20 mg/L Fe^{3+}) and a minimum I_d of 0.241 mA (at 0 mg/L Fe^{3+}). After adding 0.05 mg/L Fe^{3+}, its current response was significantly enhanced, indicating that a more effective gate area exhibits stronger I_d changes, which is applicable for the detection of trace heavy metal ions.

Sensitivity is an important indicator of the HEMT performance and can be represented by the slope of

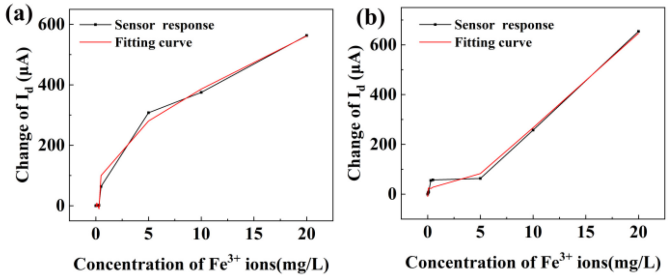

FIGURE 4. Corresponding calibration curves of a (a) conventional gate and (b) 5-fold-gate enhancement-mode HEMT sensor.

input–output characteristic curve of a sensor. Figure 4(a) shows the calibration curve based on the current response change (output) of the HEMT with a traditional structure to the added Fe^{3+} concentration (input). Using the nearly linear curve between 0.5 and 20 mg/L as the calculation interval, the calculated sensitivity for Fe^{3+} detection was 21.14 μA/(mg/L). Regarding the sensor with the 5-fold gate structure (Figure 4(b)), the linear interval of the calibration curve was between 0.3 and 20 mg/L, and the calculated sensitivity was 31.25 μA/(mg/L), much higher than that of the device with the traditional gate, which can be explained by a capacitance model of the HEMT. The V_g of the device can be expressed as:

$$V_g = \Delta V_s + \Delta V_{ca} \tag{3}$$

where ΔV_s is the voltage change in the test solution and ΔV_{ca} is the voltage change in the p-type GaN cap layer and AlGaN layer. When a test solution is dropped onto the gate, the V_g on the sensor surface changes and the voltage drop across the dielectric layer changes through the capacitance effect. The change in I_d reflects how that in V_{ca} affects the 2DEG concentration in the channel. Since the formed capacitors are combined in series, the dielectric potential can be expressed as follows [30]:

$$\Delta V_{ca} = \frac{C_s}{C_{ca} + C_s} \times V_g \tag{4}$$

where C_{ca} and C_s are the capacitance across the epitaxial layer and the solution, respectively. C_{ca} can be further expanded as:

$$C_{ca} = \frac{C_{cap} \times C_{AlGaN}}{C_{cap} + C_{AlGaN}} \tag{5}$$

where C_{cap} and C_{AlGaN} are the capacitance across the p-type GaN cap layer and AlGaN barrier layer, respectively. Since C_s is proportional to the contact area between the test solution and the gate ($C = \varepsilon A/d$), the amplitude of C_s on the sensor gate depends on the sensing area. According to Equation (4), sensors with larger gate contact areas can achieve better detection performance. Therefore, the proposed HEMT sensor with the 5-fold gate structure has advantages in the specific detection of trace Fe^{3+} and great potential in the detection of trace heavy metal ions in the future.

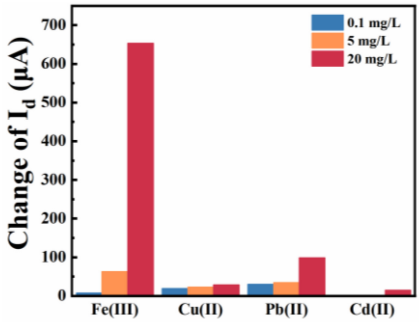

FIGURE 5. Relative current changes of the AlGaN/GaN high-electron-mobility transistor with the 5-fold gate structure for different concentrations of Fe^{3+}, Cu^{2+}, Pb^{2+}, and Cd^{2+}.

To study the specific detection of Fe^{3+} by the sensor with the 5-fold gate structure, solutions containing Fe^{3+}, Cu^{2+}, Pb^{2+}, and Cd^{2+} at concentrations of 0.1, 5, and 20 mg/L were separately dropped onto the device. Stable current responses were observed when continuously detecting for 300 s under a V_d of 7 V. Based on them, the relative current response changes for the four heavy metal ions at different concentrations were calculated (Figure 5). When the ion concentration was 0.1 mg/L, Cu^{2+} (19.83 μA) and Pb^{2+} (30.37 μA) were the main interfering ions, and their response changes were even higher than that for Fe^{3+} (8.15 μA). This may be due to the incomplete opening of the 2DEG channel, and the results might have been affected by the gate in contact with the added solution and some Si_3N_4 passivation regions. At the concentration of 5 mg/L, although Cu^{2+} (23.05 μA) and Pb^{2+} (34.48 μA) were still interfering ions, the response for Fe^{3+} (63.49 μA) was significantly the highest. When the concentration was increased to 20 mg/L, the change in the current response for Fe^{3+} (653.75 μA) was much higher than those for the other ions, indicating that the degree of binding between the modifier and these heavy metal ions was low. This demonstrates that the proposed sensor has significant specificity for Fe^{3+} and, thus, a great potential for development in Fe^{3+} detection.

IV. CONCLUSION

In this study, a 5-fold-gate enhancement-mode AlGaN/GaN HEMT with 2-mercaptobutanedioic acid functionalization was successfully prepared and compared with one having a traditional gate structure, for Fe^{3+} detection. The crystal quality of the epitaxial growth material was characterized using XRD and AFM techniques. Fe^{3+} was added dropwise to both sensors and the resulting sensitivity of the one with the traditional structure and that with the 5-fold gate was 21.14 μA/(mg/L) and 31.25 μA/(mg/L), respectively. The current response to the plasma of Fe^{3+}, Cu^{2+}, Pb^{2+}, and Cd^{2+} was used to demonstrate the sensor specificity for Fe^{3+}. The superiority of the 5-fold-gate sensor over the one with the traditional gate structure was analyzed via a capacitance model. The higher current response change and sensitivity indicate that the 2-mercaptobutanedioic-acid-modified 5-fold-gate sensor has great development prospects for the real-time specific detection of trace Fe^{3+}.

REFERENCES

[1] P. B. Tchounwou, C. G. Yedjou, A. K. Patlolla, and D. J. Sutton, "Heavy metal toxicity and the environment," *EXS*, vol. 101, pp. 133–164, Jan. 2012, doi: 10.1007/978-3-7643-8340-4_6.
[2] L. Järup, "Hazards of heavy metal contamination," *Brit. Med. Bull.*, vol. 68, no. 1, pp. 167–182, Dec. 2003, doi: 10.1093/bmb/ldg032.
[3] C. F. Carolin, P. S. Kumar, A. Saravanan, G. J. Joshiba, and M. Naushad, "Efficient techniques for the removal of toxic heavy metals from aquatic environment: A review," *J. Environ. Chem. Eng.*, vol. 5, no. 3, pp. 2782–2799, Jun. 2017, doi: 10.1016/j.jece.2017.05.029.
[4] E. M. Nolan and S. J. Lippard, "Tools and tactics for the optical detection of mercuric ion," *Chem. Rev.*, vol. 108, no. 9, pp. 3443–3480, Sep. 2008, doi: 10.1021/cr068000q.
[5] M. B. Gumpu, S. Sethuraman, U. M. Krishnan, and J. B. B. Rayappan, "A review on detection of heavy metal ions in water—An electrochemical approach," *Sensor. Actuat. B-Chem.*, vol. 213, pp. 515–533, Jul. 2015, doi: 10.1016/j.snb.2015.02.122.
[6] C. Zhang, H. Y. Jiang, Y. M. Deng, and A. H. Wang, "Adsorption performance of antimony by modified iron powder," *RSC adv.*, vol. 9, no. 54, pp. 31645–31653, Oct. 2019, doi: 10.1039/C9RA05646G.
[7] I. Sahakiants and M. Festing, "The use of executive share-based compensation in Poland: Investigating institutional and agency-based determinants in an emerging market," *Int. J. Hum. Resour. Man.*, vol. 30, no. 6, pp. 1036–1057, Mar. 2019, doi: 10.1080/09585192.2016.1172652.
[8] Y. H. Zhong, J. Li, A. Lambert, Z. J. Yang, and Q. Cheng, "Expanding the scope of chemiluminescence in bioanalysis with functional nanomaterials," *J. Mater. Chem. B*, vol. 7, no. 46, pp. 7257–7266, Dec. 2019, doi: 10.1039/C9TB01029G.
[9] Y. Huang et al., "Tracing Pb and possible correlated Cd contamination in soils by using lead isotopic compositions," *J. Hazard. Mater.*, vol. 385, Mar. 2020, Art. no. 121528, doi: 10.1016/j.jhazmat.2019.121528.
[10] H. C. Zhang et al., "Demonstration of AlGaN/GaN-based ultraviolet phototransistor with a record high responsivity over 3.6×10(7) A/W," *Appl. Phys. Lett.*, vol. 118, no. 24, Jun. 2021, Art. no. 242105, doi: 10.1063/5.0055468.
[11] F. Najafzadeh, F. Ghasemi, and M. R. Hormozi-Nezhad, "Anti-aggregation of gold nanoparticles for metal ion discrimination: A promising strategy to design colorimetric sensor arrays," *Sens. Actuators B: Chem.*, vol. 270, pp. 545–551, Oct. 2018, doi: 10.1016/j.snb.2018.05.065.
[12] G. F. Yang et al., "Surface modification of AlGaN solar-blind ultraviolet MSM photodetectors with octadecanethiol," *IEEE Trans. Elect. Dev.*, vol. 69, no. 1, pp. 195–200, Jan. 2022, doi: 10.1109/TED.2021.3125917.
[13] S. J. Pearton et al., "Recent advances in wide bandgap semiconductor biological and gas sensors," *Prog. Mater. Sci.*, vol. 55, no. 1, pp. 1–59, Jan. 2010, doi: 10.1016/j.pmatsci.2009.08.003.
[14] F. Xie, Y. Li, Y. Liu, X. Yang, X. Zhang, and G. Yang, "Effect of $C_{44}H_{30}N_4O_4$ surface modification on the performance of $Al_{0.6}Ga_{0.4}N$ MSM photodetectors," *IEEE Trans. Electron Devices*, vol. 69, no. 8, pp. 4337–4341, Aug. 2022, doi: 10.1109/TED.2022.3182285.
[15] F. Iucolano and T. Boles, "GaN-on-Si HEMTs for wireless base stations," *Mat. Sci. Semicon. Proc.*, vol. 98, pp. 100–105, Aug. 2019, doi: 10.1016/j.mssp.2019.03.032.
[16] H. C. Zhang et al., "Boosted high-temperature electrical characteristics of AlGaN/GaN HEMTs with rationally designed compositionally graded AlGaN back barriers," *Sci. China Inform. Sci.*, vol. 66, no. 8, Aug. 2023, Art. no. 182405, doi: 10.1007/s11432-022-3694-4.
[17] J. J. Komiak, "GaN HEMT: dominant force in high-frequency solid-state power amplifiers," *IEEE Microw. Mag.*, vol. 16, no. 3, pp. 97–105, Apr. 2015, doi: 10.1109/MMM.2014.2385303.
[18] A. Nigam, T. N. Bhat, S. Rajamani, S. B. Dolmanan, S. Tripathy, and M. Kumar, "Effect of self-heating on electrical characteristics of AlGaN/GaN HEMT on Si (111) substrate," *AIP Adv.*, vol. 7, no. 8, Aug. 2017, Art. no. 085015, doi: 10.1063/1.4990868.
[19] M. S. Makowski et al., "Physisorption of functionalized gold nanoparticles on AlGaN/GaN high electron mobility transistors for sensing applications," *Appl. Phys. Lett.*, vol. 102, no. 7, Feb. 2013, Art. no. 074102, doi: 10.1063/1.4791788.

[20] S. Khandelwal, N. Goyal, and T. A. Fjeldly, "A physics-based analytical model for 2DEG charge density in AlGaN/GaN HEMT devices," *IEEE Trans. Elect. Dev.*, vol. 58, no. 10, pp. 3622–3625, Oct. 2011, doi: 10.1109/TED.2011.2161314.

[21] J. Q. Niu et al., "Detection of lead ions with AlGaAs/InGaAs pseudomorphic high electron mobility transistor," *J. Semicond.*, vol. 37, no. 11, Jan. 2017, Art. no. 114003, doi: 10.1088/1674-4926/37/11/114003.

[22] L. Gu et al., "Electrical detection of trace zinc ions with an extended gate-AlGaN/GaN high electron mobility sensor," *Analyst*, vol. 144, no. 2, pp. 663–668, Jan. 2019, doi: 10.1039/C8AN01770K.

[23] Y. C. King, T. J. King, and C. M. Hu, "Charge-trap memory device fabricated by oxidation of Si1-xGex," *IEEE Trans. Elect. Dev.*, vol. 48, no. 4, pp. 696–700, Apr. 2001, doi: 10.1109/16.915694.

[24] G. N. Zhou et al., "Gate leakage suppression and breakdown voltage enhancement in p-GaN HEMTs using metal/graphene gates," *IEEE Trans. Elect. Dev.*, vol. 67, no. 3, pp. 875–880, Mar. 2020, doi: 10.1109/TED.2020.2968596.

[25] R. K. Shervedani, A. Hatefi-Mehrjardi, and A. Asadi-Farsani, "Sensitive determination of iron(III) by gold electrode modified with 2-mercaptosuccinic acid self-assembled monolayer," *Anal. Chim. Acta*, vol. 601, no. 2, pp. 164–171, Oct. 2007, doi: 10.1016/j.aca.2007.08.037.

[26] M. Vandenbossche, M. Casetta, M. Jimenez, S. Bellayer, and M. Traisnel, "Cysteine-grafted nonwoven geotextile: A new and efficient material for heavy metals sorption—Part A," *J. Environ. Manage.*, vol. 132, pp. 107–112, Jan. 2014, doi: 10.1016/j.jenvman.2013.10.027.

[27] A. Nigam, T. N. Bhat, V. S. Bhati, S. B. Dolmanan, S. Tripathy, and M. Kumar, "MPA-GSH functionalized AlGaN/GaN high-electron mobility transistor-based sensor for cadmium ion detection," *IEEE Sens. J.*, vol. 19, no. 8, pp. 2863–2870, Apr. 2019, doi: 10.1109/JSEN.2019.2891511.

[28] X. Jia, D. Chen, L. Bin, H. Lu, R. Zhang, and Y. Zheng, "Highly selective and sensitive phosphate anion sensors based on AlGaN/GaN high electron mobility transistors functionalized by ion imprinted polymer," *Sci. rep.*, vol. 6, no. 1, pp. 1–7, Jun. 2016, doi: 10.1038/srep27728.

[29] Y. Dong et al., "AlGaN/GaN heterostructure pH sensor with multi-sensing segments," *Sens. Actuators B: Chem.*, vol. 260, pp. 134–139, May 2018, doi: 10.1016/j.snb.2017.12.188.

[30] S. Mishra, P. Kachhawa, R. R. Thakur, A. K. Jain, K. Singh, and N. Chaturvedi, "Detection of heavy metal ions using meander gated GaN HEMT sensor," *Sensor. Actuat. A: Phys.*, vol. 332, Oct. 2021, Art. no. 113119, doi: 10.1016/j.sna.2021.113119.